

Knockdown of lncRNA HOXA-AS3 Suppresses the Progression of Atherosclerosis via Sponging miR-455-5p

This article was published in the following Dove Press journal:
Drug Design, Development and Therapy

Kui Chi¹
Jinwen Zhang¹
Huanhuan Sun¹
Yang Liu¹
Ye Li²
Tao Yuan¹
Feng Zhang¹

¹Department of Vascular Surgery, The Second Hospital of Hebei Medical University, Shijiazhuang, Hebei 050000, People's Republic of China; ²Department of Anesthesiology, The Second Hospital of Hebei Medical University, Shijiazhuang, Hebei 050000, People's Republic of China

Background: Atherosclerosis can lead to multiple cardiovascular diseases, especially myocardial infarction. Long noncoding RNAs (lncRNAs) are involved in multiple diseases, including atherosclerosis. lncRNA HOXA-AS3 was found to be notably upregulated in atherosclerosis. However, the biological function of HOXA-AS3 during the occurrence and development of atherosclerosis remains unclear.

Materials and Methods: Human vascular endothelial cells (HUVECs) were treated with oxidized low-density lipoprotein (oxLDL) to mimic atherosclerosis in vitro. Gene and protein expressions in HUVECs were detected by RT-qPCR and Western blot, respectively. Cell proliferation was tested by CCK-8 and Ki67 staining. Cell apoptosis and cycle were measured by flow cytometry. Additionally, the correlation between HOXA-AS3 and miR-455-5p was confirmed by dual luciferase report assay and RNA pull-down. Finally, in vivo model of atherosclerosis was established to confirm the function of HOXA-AS3 during the development of atherosclerosis in vivo.

Results: lncRNA HOXA-AS3 was upregulated in oxLDL-treated HUVECs. In addition, oxLDL-induced growth inhibition of HUVECs was significantly reversed by knockdown of HOXA-AS3. Consistently, oxLDL notably induced G1 arrest in HUVECs, while this phenomenon was greatly reversed by HOXA-AS3 siRNA. Furthermore, downregulation of HOXA-AS3 notably inhibited the progression of atherosclerosis through mediation of miR-455-5p/p27 Kip1 axis. Besides, silencing of HOXA-AS3 notably relieved the symptom of atherosclerosis in vivo.

Conclusion: Downregulation of HOXA-AS3 significantly suppressed the progression of atherosclerosis via regulating miR-455-5p/p27 Kip1 axis. Thus, HOXA-AS3 might serve as a potential target for the treatment of atherosclerosis.

Keywords: atherosclerosis, lncRNA HOXA-AS3, miR-455-5p, p27 Kip1

Introduction

Atherosclerosis is one of the leading causes of myocardial infarction in the world.¹ In fact, atherosclerosis is a multistep disease, which results from multiple risk factors,^{2,3} including dysfunction of HUVECs.⁴ Various dysfunctions of HUVECs including inappropriate proliferation, migration and apoptosis are critical cellular events resulting in the occurrence and development of atherosclerosis.⁵ Therefore, the function of HUVECs is crucial for the treatment of atherosclerosis.

Many reports have considered noncoding RNAs (ncRNAs) as possible regulators of multiple diseases.^{6,7} The ncRNAs, greater than 200 nucleotides in length

Correspondence: Feng Zhang
Email zhangfeng_12@126.com

with limited or no protein-coding capacity are known as long non-coding RNAs (lncRNAs).⁸ lncRNAs have been regarded to play a key role in progression of multiple diseases, including atherosclerosis.^{9,10} Wang et al found that lncRNA MALAT1 could promote autophagy in HUVECs by sponging miR-216a-5p.¹¹ Additionally, Cui et al indicated that lncRNA 430,945 promoted the proliferation and migration of vascular smooth muscle cells via regulating ROR2/RhoA signaling pathway in atherosclerosis.¹² Previous studies have indicated that HOXA-AS3 could significantly mediate the progression of multiple diseases.^{10,13} In addition, HOXA-AS3 was found to be notably upregulated in atherosclerosis.¹⁰ However, the function of HOXA-AS3 in atherosclerosis remains unclear. Based on these backgrounds, this research aimed to explore the biological function of HOXA-AS3 during the progression of atherosclerosis in vitro and in vivo.

Materials and Methods

Cell Culture and Treatment

HUVECs were obtained from American Type Culture Collection (ATCC, Manassas, VA, USA) and cultured in RPMI-1640 medium, supplemented with 10% FBS and 2 mM Glutamine (Sigma Aldrich, St. Louis, MO, USA) at 37°C. To mimic in vitro model of atherosclerosis, HUVECs were treated with 100 ng/mL oxidized low-density lipoprotein (oxLDL) for 48 h according to the previous studies.^{14,15}

Cell Transfection

SiRNAs against HOXA-AS3 (HOXA-AS3 siRNA1, HOXA-AS3 siRNA2 and HOXA-AS3 siRNA3, 10 nM) were purchased from Riobo company and transfected into HUVECs using Lipofectamine[®] 2000 (Thermo Fisher Scientific, Inc.) according to the manufacturer's instructions. The efficiency of transfection was detected by reverse transcription-quantitative PCR (RT-qPCR).

For miR-455-5p transfection, HUVECs were transfected with 10 nM miR-455-3p agomir, miR-455-5p antagomir or NC by Lipofectamine 2000 according to the previous reference.¹⁶ MiR-455-5p agomir, antagomir and negative control RNAs were purchased from GenePharma (Shanghai, China).

Quantitative Real-Time Polymerase Chain Reaction (RT-qPCR)

Total RNAs were extracted from cell lines with TRIZOL reagent (Invitrogen, Carlsbad, CA, USA). We carried out reverse transcription and real-time PCR assays by means of PrimeScript RT reagent Kit (Takara, Tokyo, Japan) and SYBR premix Ex Taq II kit (Takara, Tokyo, Japan) severally. β -actin or U6 was used as the internal control. The primers for lncRNA HOXA-AS3 were: forward: 5'-GGTAAACCGGGCTCGTGTAC-3' and reverse: 5'-ATTCAGCCAGAGTTCTCCGC-3'; the primers for p27 Kip1 were: forward: 5'-TAACTCTGAGGACACGCA TTTG-3' and reverse: 5'-GTTTTGAGTAGAAG AATCGTCGG-3'; the primers for miR-455-5p were: forward: 5'-TTGGACTACATCGCTCAACTGA-3' and reverse: 5'-CTCAACTGGTGTCTGGAGTC-3'; the primers for U6 were: forward: 5'-CTCGCTTCGGCAGC ACAT-3' and reverse: 5'-AACGCTTCACGAATTTGCGT -3' and the primers for β -actin were: forward: 5'-GTCCACCGCAAATGCTTCTA-3' and reverse: 5'-TGCTGTCACCTTCACCGTTC-3'. $2^{-\Delta\Delta CT}$ method was utilized to measure the relative expression.

CCK-8 Assay

HUVECs cells were seeded in 96-well plates (5×10^3 per well) overnight. Then, cells were treated with 100 μ g/mL oxLDL, HOXA-AS3 siRNA2 or oxLDL + HOXA-AS3 siRNA2 for 0, 24, 48 and 72 h, respectively. 10 μ L CCK-8 reagents (Beyotime, Shanghai, China) were added to each well and cells were incubated for 2 h at 37°C. Finally, the absorbance of HUVECs was measured at 450 nm using a microplate reader (Thermo Fisher Scientific).

RNA Pull-Down

For RNA pulldown assay, the Biotin RNA Labeling Mix (Roche, Basel, Switzerland) was used to transcribe and label probe-control or probe-HOXA-AS3 in vitro. An RNA structure buffer (Thermo, MA, USA) was used to induce secondary structure formation from the biotin-labeled RNAs. Streptavidin beads (Thermo) were washed three times with 500 μ L of RNA immunoprecipitation wash buffer (Thermo Fisher Scientific) and then added to the biotinylated RNAs at 4°C overnight. The overnight mixture was separated by a magnetic field so that streptavidin bead-RNA complexes could be obtained. Then, lysates of HUVECs were added to the

complexes and incubated on a rotator at room temperature for one hour. The incubated mixture was again separated with a magnetic field so that streptavidin bead-RNA-protein complexes could be obtained.

Cell Cycle Detection

Cell cycle was determined by flow cytometry using Cycle Detection Kit I (BD Biosciences, Franklin Lake, NJ, USA). After 24 hours of transfection, cells were lifted and fixed in pre-cold 70% ethanol at 4°C overnight. Then, cells were treated with 100 μ L propidium iodide (PI)/RNase Staining Buffer (Thermo Fisher Scientific, Waltham, MA, USA) at room temperature in the dark for 30 min. Finally, Flow cytometry (BD Biosciences, Franklin Lake, NJ, USA) was used to detect the cell cycle distribution and the data were analyzed using the Flowjo software (BD, Franklin Lake, NJ, USA).

In vitro Angiogenesis Assay

For angiogenesis assay, 6-well plates were pre-coated with matrigel (BD Biosciences, San Jose, CA, USA). Then, 1×10^5 HUVECs cells were seeded into each well. After 24 h of culturing at 37°C, the formation of capillary-like structures was photographed and the branch points were counted. The tube length was analyzed by the AxioVision Rel software version 4.8 (Carl Zeiss AG, Jena, Germany).

Western Blotting

Total protein was isolated from cell lysates by using RIPA buffer, and quantified by BCA protein assay kit (Beyotime, Shanghai, China). Proteins were resolved on 10% SDS-PAGE and then transferred onto PVDF (Bio-Rad) membranes. After blocking with 5% skim milk in TBST for 1 h, the membranes were incubated with primary antibodies at 4°C overnight. Then, the membranes were incubated with secondary anti-rabbit antibody (Abcam; 1:5000) at room temperature for 1 h. Membranes were scanned by using an Odyssey Imaging System and analyzed with Odyssey v2.0 software (LICOR Biosciences, Lincoln, NE, USA). The primary antibodies used in this study were as follows: anti-p27 Kip1 (Abcam, Cambridge, MA, USA; 1:1000), anti-Bax (Abcam; 1:1000), anti-cleaved caspase 3 (Abcam; 1:1000), anti-Bcl-2 (Abcam; 1:1000), anti-cleaved caspase 9 (Abcam; 1:1000), anti-CDK2 (Abcam; 1:1000), anti-Cyclin E1 (Abcam; 1:1000) and anti- β -actin (Abcam; 1:1000). β -actin was used as an internal control.

Measurement of Mitochondrial Membrane Potential (MMP) ($\Delta\psi_m$)

Changes in mitochondrial membrane potential (MMP) were measured with JC-1 (5,5',6,6'-Tetrachloro-1,1',3,3'-tetraethyl-imidacarbocyanine) staining on the FACScan flow cytometer. Briefly, cells were plated into 6-well plates (3×10^5 cells/well) overnight. Cells were harvested, washed twice with PBS, and then resuspended in 0.5 ml of complete medium containing 2 μ M JC-1 at 37°C for 20 min. Finally, the data were analyzed using the flow cytometer in the FL1 and FL2 channels.

Immunofluorescence

HUVECs were seeded in 24-well plates overnight. Then, cells were treated with NC or HOXA-AS3 siRNA2 for 72 h. Next, cells were blocked with 10% goat serum for 30 min at room temperature and then incubated with anti-Ki67 antibody (Abcam, Cambridge, MA, USA; 1:1000) at 4°C overnight, followed by incubation with goat anti-rabbit IgG (Abcam; 1:5000) at 37°C for 1 h. Then, the nuclei were stained with DAPI (Beyotime, Shanghai, China) for 5 min. Finally, cells were observed under a fluorescence microscope (Olympus CX23, Tokyo, Japan).

Cell Apoptosis Analysis

HUVECs were trypsinized, washed with phosphate buffered saline and resuspended in Annexin V Binding Buffer. Then, cells were stained with 5 μ L FITC and 5 μ L propidium (PI) for 15 min. After that, cells were analyzed using flow cytometer (BD, Franklin Lake, NJ, USA) to test the cell apoptosis rate.

Dual Luciferase Reporter Assay

The partial sequences of HOXA-AS3 and 3'-UTR of p27 Kip1 containing the putative binding sites of miR-455-5p were synthesized and obtained from Sangon Biotech (Shanghai, China), which were then cloned into the pmirGLO Dual-Luciferase miRNA Target Expression Vectors (Promega, Madison, WI, USA) to construct wild-type or mutate type reporter vectors HOXA-AS3 (WT/MT) and p27 Kip1 (WT/MT), respectively. The HOXA-AS3 (WT/MT) or p27 Kip1 (WT/MT) were transfected into HUVECs together with control, vector-control (NC) or miR-455-5p agomir using Lipofectamine 2000 (Thermo Fisher Scientific) according to the manufacturer's instructions. The relative luciferase activity was analyzed by the Dual-Glo Luciferase Assay System (Promega).

In vivo Experiment

Fifteen male ApoE^{-/-} mice (aged 7 weeks) were purchased from Vital River (Beijing, China) and divided into 3 groups: control, high-fat diet (HFD) and HFD + HOXA-AS3 Lenti-siRNA2. Mice in control group were fed with normal diet. In order to mimic in vivo model of atherosclerosis, mice in other groups were fed with HFD (1.25% cholesterol and 20% lard) for 10 weeks. A HOXA-AS3 knockdown mouse model was constructed by injecting a lentivirus (Lenti) expressing RNA interference (RNAi) targeting HOXA-AS3 (HOXA-AS3 Lenti-siRNA2), which was purchased from Genepharma (Shanghai, China). In addition, HOXA-AS3 Lenti-siRNA2 was injected into the tail vein of mice in HFD + HOXA-AS3 Lenti-siRNA2 group according to a previous study.¹⁷ At the end of the study, mice were sacrificed for collection of arterial tissues and serum. The levels of triglyceride (TG), total cholesterol (TC) and LDL cholesterol (LDL-C) in mice were detected by Blood Lipid Biochemistry Kit (Beyotime, Shanghai, China). All mice were housed under specific pathogen-free (SPF) conditions of Hebei Medical University. All in vivo experiments were performed in accordance with National Institutes of Health guide for the care and use of laboratory animals, following a protocol approved by the Ethics Committees of Hebei Medical University.

H&E Staining of Coronary Artery

The arterial tissues of mice were fixed with 4% paraformaldehyde (PFA) and then embedded in paraffin. Further, they were sliced latitudinally, stained by hematoxylin-eosin (H&E), and finally shot by a digital microscope (magnification: ×100).

Statistical Analysis

Data are presented as the mean ± SD. The comparison between two groups was analyzed using Student's *t*-test. Comparisons among multiple groups were made using ANOVAs followed by Tukey's test using the Graphpad Prism 7 (La Jolla, CA, USA). *P*<0.05 was considered to indicate a statistically significant difference.

Results

OxLDL-Induced Growth Inhibition of HUVECs Was Significantly Reversed by HOXA-AS3 Knockdown

To mimic atherosclerosis in vitro, HUVECs were treated with different concentrations of oxLDL (50, 75 or 100

μg/mL). As indicated in Figure 1A, the expression of HOXA-AS3 in HUVECs was significantly upregulated by oxLDL in a dose-dependent manner. Based on this data, 100 μg/mL of oxLDL was selected of use in the following experiments. Next, the transfection efficiency of HOXA-AS3 siRNAs was detected by RT-qPCR. The results demonstrated that expression of HOXA-AS3 in HUVECs was notably downregulated in the presence of HOXA-AS3 siRNAs (Figure 1B). Since HUVECs were more sensitive to HOXA-AS3 siRNA2, HOXA-AS3 siRNA2 was selected for use. In addition, CCK-8 assay indicated that the viability of HUVECs was notably suppressed by oxLDL, while this phenomenon was reversed in the presence of HOXA-AS3 siRNA2 (Figure 1C). Consistently, the data of Ki67 staining confirmed that knockdown of HOXA-AS3 significantly inhibited the anti-proliferative effect of oxLDL in HUVECs (Figure 1D). Altogether, oxLDL-induced growth inhibition of HUVECs was significantly reversed by HOXA-AS3 siRNA2.

HOXA-AS3 Sponged miR-455-5p in HUVECs

In order to explore the mechanism by which HOXA-AS3 mediated the growth of HUVECs, starbase (<http://starbase.sysu.edu.cn/>) and miRDB (<http://www.mirdb.org/>) were used. As demonstrated in Figure 2A, HOXA-AS3 had a putative targeting site of miR-455-5p. In addition, RT-qPCR was performed to detect the efficiency of miRNA transfection. As we expected, the miR-455-5p agomir or antagomir was stably transfected into HUVECs (Figure 2B). Furthermore, co-transfection of the wild-type HOXA-AS3 vector (WT-HOXA-AS3) with miR-455-5p agomir significantly reduced luciferase activities compared with mutant HOXA-AS3 vector (MT-HOXA-AS3, Figure 2C). Besides, the result of RNA pull-down further verified that HOXA-AS3 bound to miR-455-5p (Figure 2D). Taken together, HOXA-AS3 could sponge miR-455-5p in HUVECs.

HOXA-AS3 siRNA2 Notably Suppressed oxLDL-Induced Apoptosis of HUVECs via Sponging miR-455-5p

Next, JC-1 staining was performed to detect the effect of HOXA-AS3 on mitochondrial membrane potential in vitro. The data revealed that knockdown of HOXA-AS3 significantly relieved the mitochondrial injury in

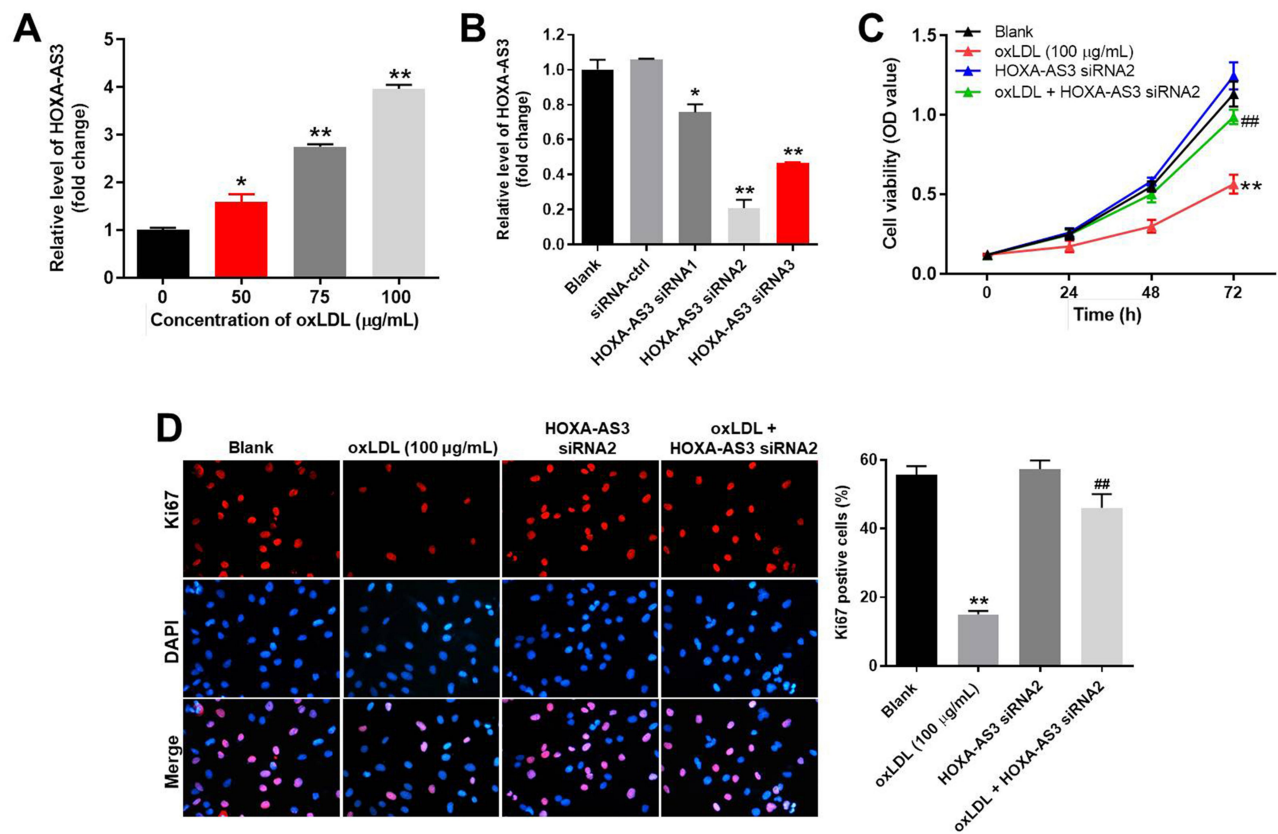


Figure 1 OxLDL-induced growth inhibition of HUVECs was significantly reversed by HOXA-AS3 knockdown. (A) HUVECs were treated with 0, 50, 75 or 100 µg/mL oxLDL for 48 h. Then, the expression of HOXA-AS3 in HUVECs was detected by RT-qPCR. (B) HUVECs were transfected with HOXA-AS3 siRNA1, siRNA2 or siRNA3 for 24 h. Then, the expression of HOXA-AS3 in HUVECs was measured by RT-qPCR. (C) HUVECs were treated with oxLDL (100 µg/mL), HOXA-AS3 siRNA2 or oxLDL + HOXA-AS3 siRNA2 for 0, 24, 48 or 72 h. The viability of HUVECs was detected by CCK-8 assay. (D) The proliferation of HUVECs was detected by Ki67 staining. The Ki67 positive rate was calculated. Red immunofluorescence indicated Ki67. Blue immunofluorescence indicated DAPI. * $P < 0.05$ compared to control, ** $P < 0.01$ compared to control, ### $P < 0.01$ compared to oxLDL (100 µg/mL); $n = 3$.

oxLDL-treated HUVECs. However, the protective effect of HOXA-AS3 on mitochondrial membrane potential was partially abolished in the presence of miR-455-5p antagomir (Figure 3A). In addition, flow cytometry was used to detect the cell apoptosis. The data revealed that oxLDL-induced apoptosis of HUVECs was significantly suppressed by HOXA-AS3 siRNA2, while this anti-apoptotic effect was partially abolished by miR-455-5p antagomir (Figure 3B). However, HOXA-AS3 siRNA2 alone had very limited effect on apoptosis of HUVECs (Figure 3B). Meanwhile, Western blot data indicated the expressions of pro-apoptotic proteins (Bax, cleaved caspase 3 and cleaved caspase 9) in oxLDL-treated HUVECs were greatly inhibited by HOXA-AS3 knockdown (Figure 3C–G). In contrast, oxLDL-induced anti-apoptotic protein (Bcl-2) decrease was notably reversed in the presence of HOXA-AS3 siRNA2 (Figure 3C–G). Consistently, the effect of HOXA-AS3 siRNA2 on these proteins was partially abrogated by miR-455-5p

antagomir. All these results revealed that HOXA-AS3 siRNA2 notably suppressed oxLDL-induced apoptosis of HUVECs via sponging miR-455-5p.

HOXA-AS3 Knockdown Obviously Inhibited the Progression of Angiogenesis *in vitro*

For the purpose of exploring the role of HOXA-AS3 in atherosclerosis, angiogenesis assay was performed. As revealed in Figure 4A and B, the branch points of capillary-like structures in oxLDL-treated HUVECs were significantly decreased, while this phenomenon was greatly improved in the presence of HOXA-AS3 siRNA2. Similarly, oxLDL-induced decrease of the tube length of HUVECs was greatly reversed by silencing of HOXA-AS3, while the protective effect of HOXA-AS3 siRNA2 on tube length was partially abolished by miR-455-5p antagomir (Figure 4C). Altogether, HOXA-AS3

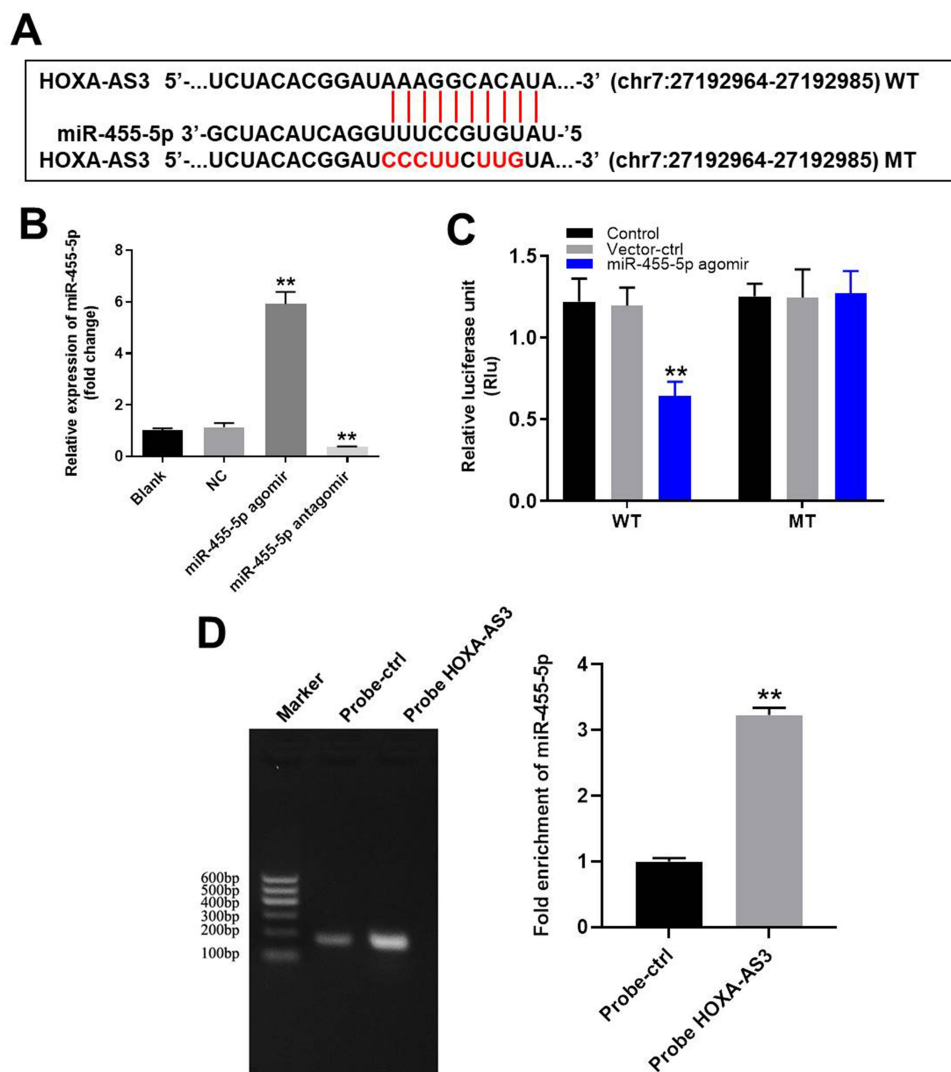


Figure 2 HOXA-AS3 sponged miR-455-5p in HUVECs. **(A)** Gene structure of HOXA-AS3 indicated the predicted target site of miR-455-5p in its 3'UTR. **(B)** HUVECs were transfected with 10 μ M miR-455-5p agomir or antagomir. Then, the efficiency of transfection was verified by RT-qPCR. **(C)** The luciferase activity was measured in HUVECs following co-transfecting with WT/MT HOXA-AS3 3'-UTR plasmid and miR-455-5p with the dual luciferase reporter assay. **(D)** RNA pull-down was performed to verify the correlation between HOXA-AS3 and miR-455-5p. ** $P < 0.01$ compared with control; $n = 3$.

knockdown obviously inhibited the progression of angiogenesis in vitro.

MiR-455-5p Directly Targeted P27 Kip1

To find the direct mRNA target of miR-455-5p, targetscan (http://www.targetscan.org/vert_71/) and dual luciferase report assay were performed. As indicated in Figure 5A and B, p27 Kip1 might be the target of miR-455-5p. Next, RT-qPCR and Western blot were performed to verify this data. As we expected, the expression of p27 Kip1 in HUVECs was significantly downregulated in the presence of miR-455-5p agomir (Figure 5C–E). All these data confirmed that miR-455-5p directly targeted p27 Kip1.

HOXA-AS3 Mediated the Cycle Distribution of HUVECs via Sponging miR-455-5p

Since p27 Kip1 played a key role in cell cycle,¹⁸ flow cytometry was used to detect cell cycle. As shown in Figure 6A, oxLDL-induced G1 arrest of HUVECs was significantly reversed by HOXA-AS3 siRNA2, while this phenomenon was abolished by miR-455-5p antagomir. Additionally, oxLDL-induced upregulation of p27 Kip1 in HUVECs was significantly reversed by HOXA-AS3 siRNA2 (Figure 6B and C). Consistently, oxLDL-induced decrease of CDK2 and cyclin E1 expressions in HUVECs was notably reversed by HOXA-AS3 siRNA2

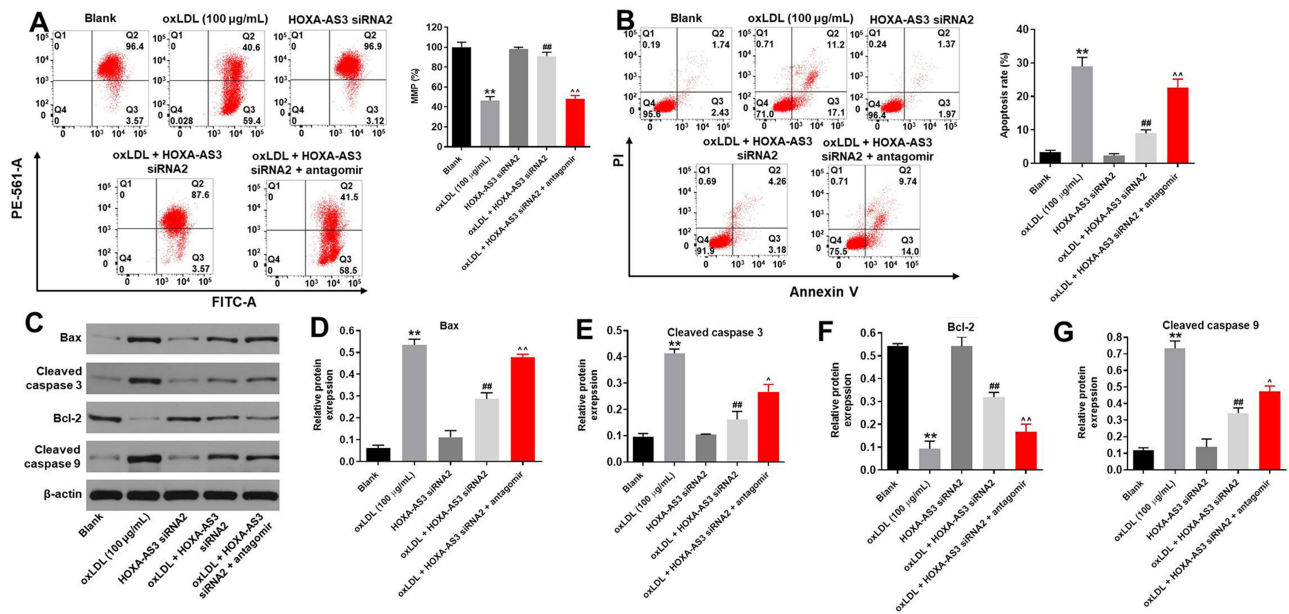


Figure 3 HOXA-AS3 siRNA2 notably suppressed oxLDL-induced apoptosis of HUVECs via sponging miR-455-5p. HUVECs were treated with oxLDL (100 µg/mL), oxLDL + HOXA-AS3 siRNA2 or oxLDL + HOXA-AS3 siRNA2 + miR-455-5p antagonist. **(A)** Changes in mitochondrial membrane potential (MMP) were measured with JC-1 staining on the FACS flow cytometer. The ratio of mitochondrial membrane potential (MMP) was calculated. **(B)** Cell apoptosis was detected with Annexin V/PI staining. The rate of apoptotic cells was detected by FACS. X axis: the level of Annexin-V FITC fluorescence; Y axis: the PI fluorescence. **(C)** The protein expressions of Bax, cleaved caspase 3, Bcl-2, cleaved caspase 9 in HUVECs were detected by Western blot. **(D)** The relative expression of Bax was quantified via normalizing to β-actin. **(E)** The relative expression of cleaved caspase 3 was quantified via normalizing to β-actin. **(F)** The relative expression of Bcl-2 was quantified via normalizing to β-actin. **(G)** The relative expression of cleaved caspase 9 was quantified via normalizing to β-actin. **P<0.01 compared with control, ###P<0.01 compared to oxLDL (100 µg/mL), ^P<0.05, ^^P<0.01 compared to oxLDL (100 µg/mL) + HOXA-AS3 siRNA2; n = 3.

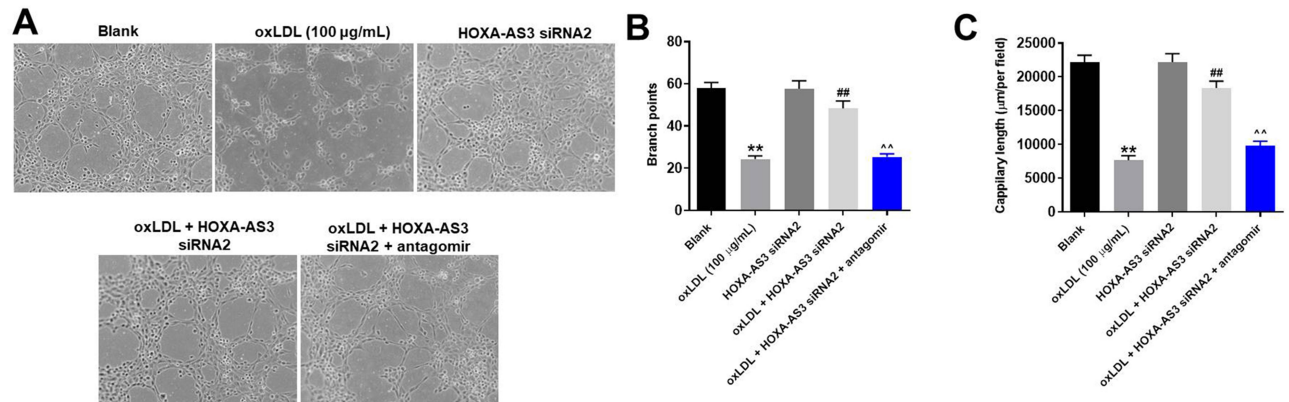


Figure 4 HOXA-AS3 knockdown obviously inhibited the progression of angiogenesis in vitro. **(A)** The formation of capillary-like structures was photographed in HUVECs was pictured. **(B)** The branch points were calculated. **(C)** The capillary length was tested. **P<0.01 compared with control, ###P<0.01 compared to oxLDL (100 µg/mL), ^^P<0.01 compared to oxLDL (100 µg/mL) + HOXA-AS3 siRNA2; n = 3.

(Figure 6B, D and E) as well. Consistently, the effect of HOXA-AS3 siRNA2 on these proteins was partly abrogated by miR-455-5p antagonist (Figure 6B, D and E). All these data confirmed that HOXA-AS3 mediated the cycle distribution of HUVECs via sponging miR-455-5p.

HOXA-AS3 siRNA2 Significantly Alleviated the Symptom of Atherosclerosis in vivo

In order to confirm the role of HOXA-AS3 in atherosclerosis, in vivo mouse atherosclerosis model was established. As indicated in Figure 7A, thickened coronary wall

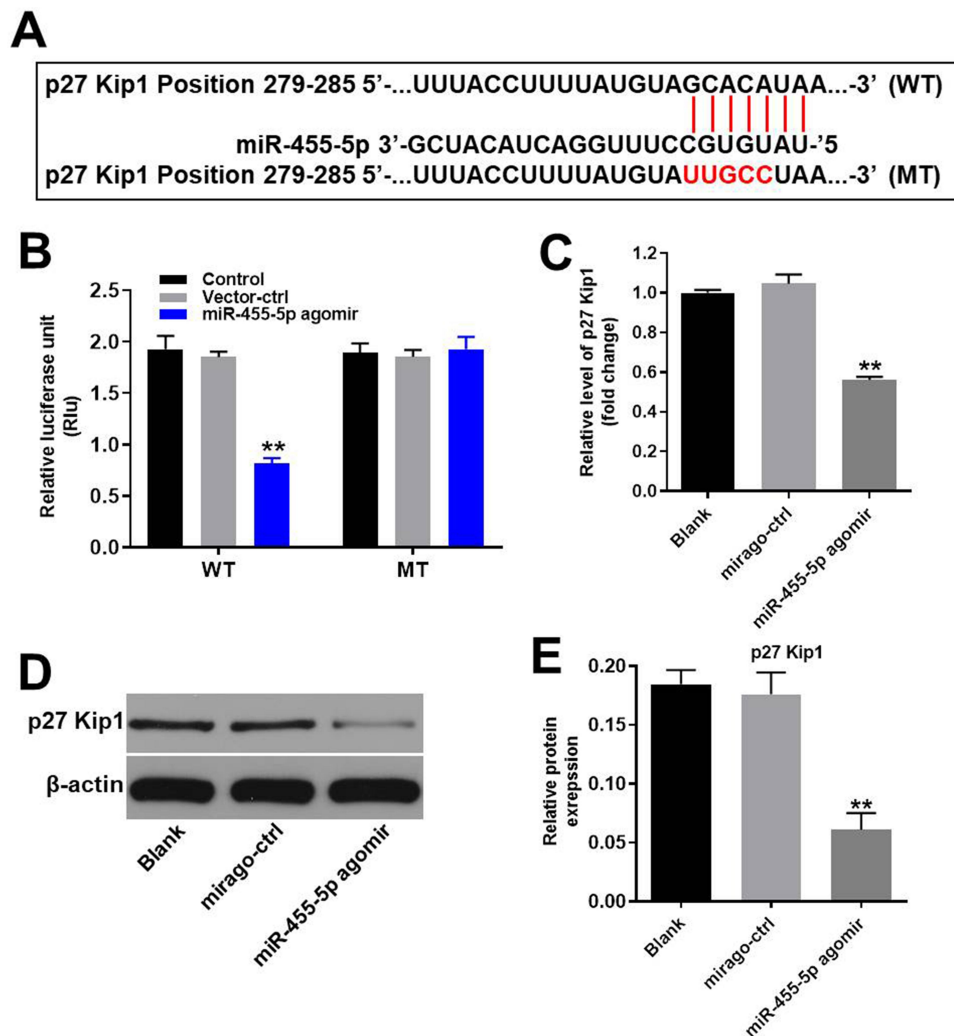


Figure 5 MiR-455-5p directly targeted p27 Kip1. (A) Gene structure of p27 Kip1 at the position of 279–285 indicates the predicted target site of miR-455-5p in its 3'UTR. (B) The luciferase activity was measured after co-transfecting with WT/MT p27 Kip1 3'-UTR plasmid and miR-455-5p agomir in HUVECs using the dual luciferase reporter assay. The results were normalized to Renilla luciferase. (C) HUVECs were transfected with miR-455-5p agomir or NC for 24 h. Then, the expression of p27 Kip1 in HUVECs was detected by RT-qPCR. (D) Protein expression of p27 Kip1 in HUVECs was detected by Western blot. (E) The relative expression of p27 Kip1 was quantified via normalization to β-actin. ** $P < 0.01$ vs. control group; $n = 3$.

in mice was observed after treatment of HFD. However, knockdown of HOXA-AS3 ameliorated the pathological change of coronary wall (Figure 7A). In addition, the levels of TG, TC and LDL-C in serum of mice were significantly upregulated by HFD, which were notably rescued in the presence of Lenti-HOXA-AS3 siRNA2 (Figure 7B–D). To sum up, silencing of HOXA-AS3 significantly alleviated the symptom of atherosclerosis in vivo.

Discussion

Previous studies have revealed that lncRNAs played an important role in the development of atherosclerosis.^{6,7} In the present study, we found that HOXA-AS3 was

significantly upregulated in oxLDL treated HUVECs in vitro. Some reports have found that HOXA-AS3 was involved in multiple diseases.^{13,19} For example, HOXA-AS3 could promote NF-κB signaling to regulate endothelium inflammation.¹⁰ Our current study firstly explored the biological function of HOXA-AS3 on atherosclerosis, suggesting that HOXA-AS3 might act as a promoter during the occurrence of atherosclerosis.

Next, we further investigate the mechanism by which HOXA-AS3 knockdown suppressed the progression of atherosclerosis. The data of dual luciferase report assay revealed that miR-455-5p was the downstream target gene of HOXA-AS3. As we knew, miRNAs have been regarded to be highly conserved ncRNAs that exhibit multiple

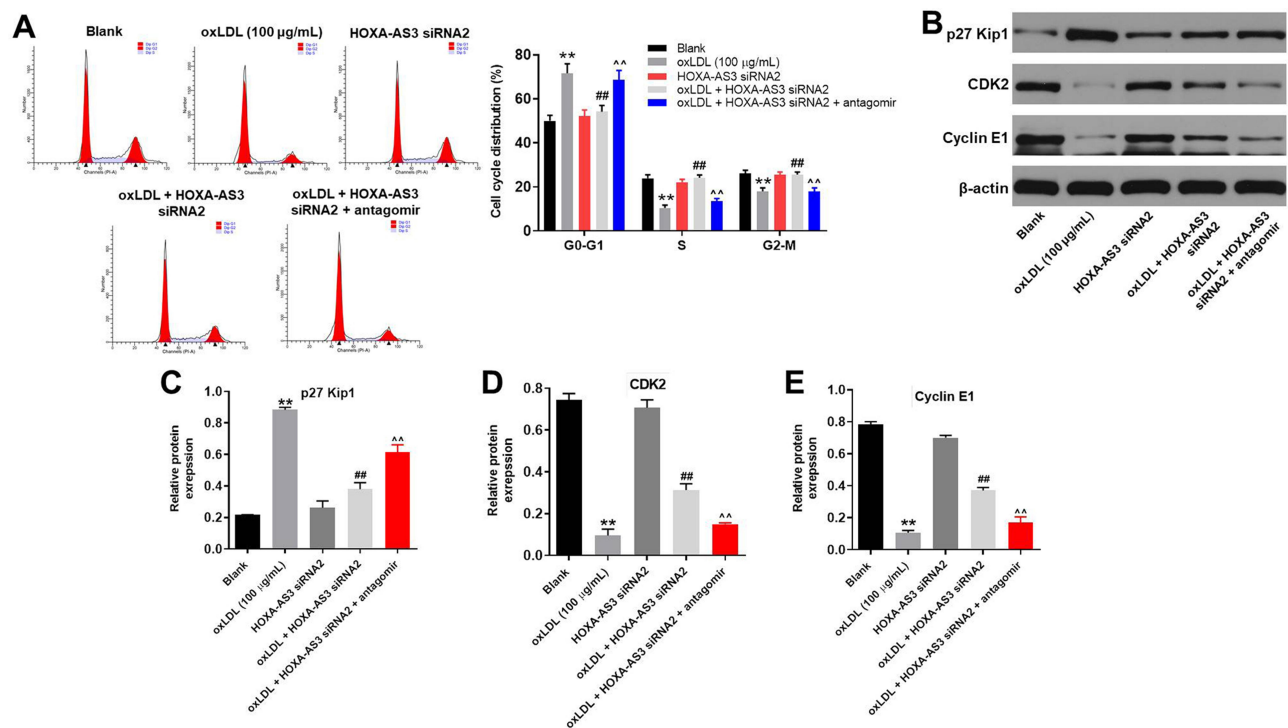


Figure 6 HOXA-AS3 mediated the cycle of HUVECs via sponging miR-455-5p. **(A)** The cell cycle distribution in G0/G1, S, and G2 phase after propidium iodide (PI) staining of HUVECs were determined by FACS. **(B)** The expressions of p27 Kip1, CDK2 and Cyclin E1 in HUVECs were detected by Western blot. **(C)** The relative expression of p27 Kip1 was quantified via normalizing to β -actin. **(D)** The relative expression of CDK2 was quantified via normalizing to β -actin. **(E)** The relative expression of Cyclin E1 was quantified via normalizing to β -actin. ** $P < 0.01$ compared with control, ## $P < 0.01$ compared to oxLDL (100 $\mu\text{g/mL}$), ^^ $P < 0.01$ compared to oxLDL (100 $\mu\text{g/mL}$) + HOXA-AS3 siRNA2; $n = 3$.

biological functions.^{20,21} Recent studies suggested that miR-455-5p could regulate various kinds of diseases.^{22,23} Our research firstly found the function of miR-455-5p on atherosclerosis, supplementing the biological role of miR-455-5p during the progression of atherosclerosis.

To further explore the biological role of HOXA-AS3 during the development of atherosclerosis, in vitro experiments were performed. We found that downregulation of HOXA-AS3 could inhibit the apoptosis of HUVECs induced by oxLDL. Moreover, HOXA-AS3 knockdown greatly suppressed the expressions of Bax, cleaved caspase 9 and cleaved caspase 3 and increased the protein level of Bcl-2. Bax, cleaved caspase 3, cleaved caspase 9 and Bcl-2 were key regulators of cell apoptosis.^{24–26} Bax, cleaved caspase 9 and cleaved caspase 3 have been considered to be the pro-apoptotic protein during the cell apoptosis, while upregulation of Bcl-2 could inhibit the apoptosis of cells.^{20,27} Our data were consistent with these backgrounds, indicating that HOXA-AS3 silencing suppressed the apoptosis of HUVECs via inhibiting Bax, cleaved caspase 9 and cleaved caspase 3 expressions.

It has been regarded that miRNAs exert their biological functions which result from their target genes.²¹ In this research, we firstly found that p27 Kip1 was identified as a direct target of miR-455-5p in atherosclerosis. P27 Kip1 has been regarded as a cell cycle regulator firstly confirmed as a cyclin-dependent kinase antagonist.²⁸ It has been confirmed that silencing of lncRNA UCA1 could curb cell proliferation and accelerate cell apoptosis via regulation of p27 Kip1.²⁹ Additionally, LINC-01572:28 could inhibit granulosa cell growth via a decrease in p27 Kip1.³⁰ In our study, downregulation of HOXA-AS3 significantly decreased the protein level of p27 Kip1. Our findings were consistent with the previous studies. Collectively, our findings revealed that HOXA-AS3 knockdown exhibited therapeutic effect on atherosclerosis via indirectly targeting p27 Kip1. Otherwise, a previous report has suggested that miR-455-5p could suppress the growth and invasion of hepatocellular carcinoma cells through targeting insulin growth factor receptor (IGF-1R).³¹ This difference may be due to the different diseases.

Moreover, in vitro experiments indicated that silencing of HOXA-AS3 notably inhibited G1 arrest in oxLDL-treated

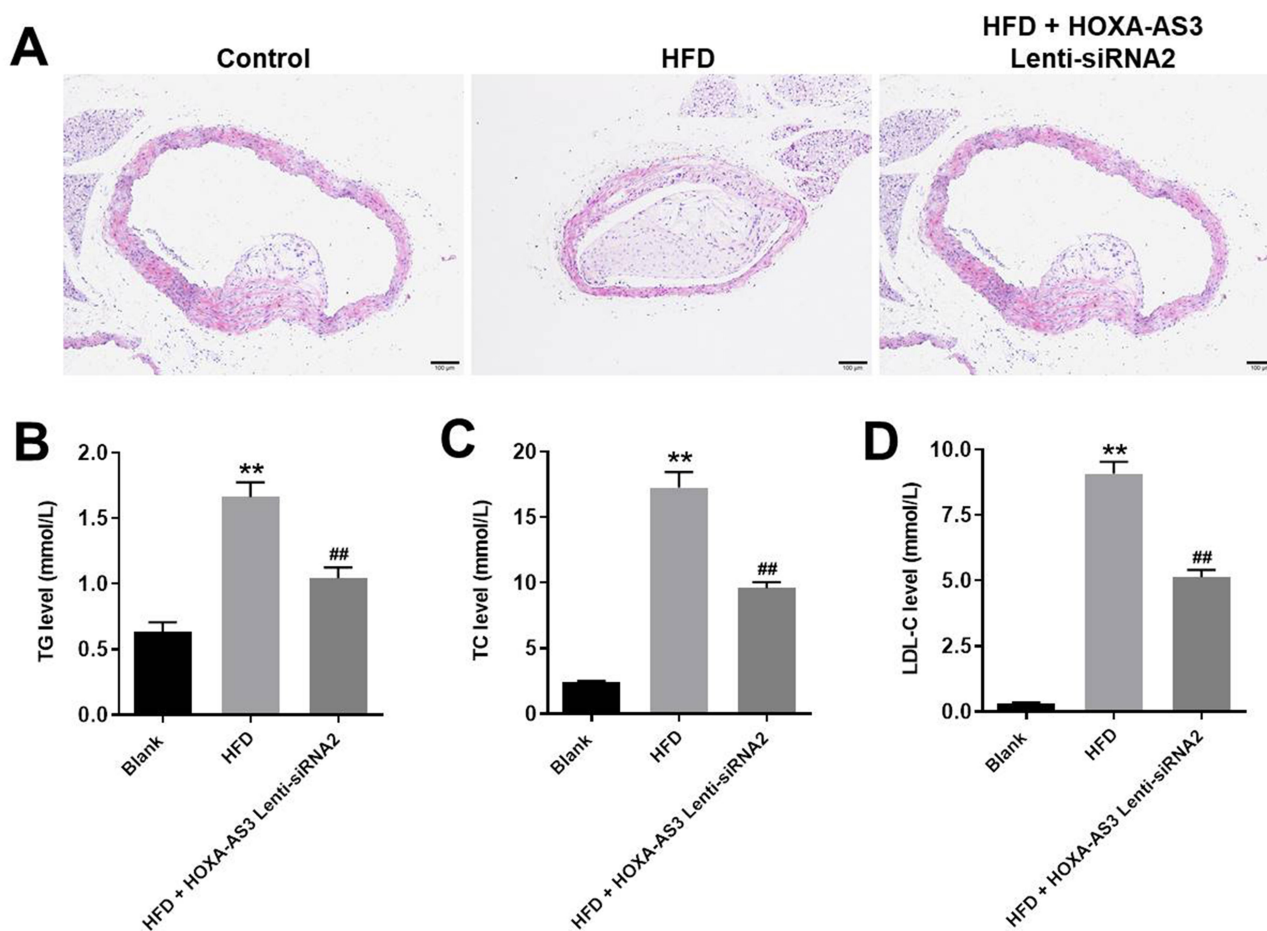


Figure 7 HOXA-AS3 siRNA2 significantly alleviated the symptom of atherosclerosis in vivo. Mice were sacrificed at the end of the study and then the arterial tissues and serum were collected. **(A)** The pathologic condition of the coronary artery was analyzed by H&E (magnification: $\times 100$). The levels of **(B)** TG, **(C)** TC and **(D)** LDL-C in serum of mice were detected by Blood Lipid Biochemistry Kit. ** $P < 0.01$ compared with Blank, ### $P < 0.01$ compared with HFD; $n = 5$.

HUVECs via upregulating the expression of CDK2 and cyclin E1. CDK2 and cyclin E1 have been considered to be cell cycle regulators in multiple diseases.^{32,33} Furthermore, Tian et al found that upregulation of miR-154-5p induced cell cycle arrest in osteosarcoma via downregulation of CDK2.³⁴ Overexpression of Monocyte chemoattractant protein-1-induced protein 1 (MCP1) could inhibit the progression of human neuroblastoma through suppression of cyclin E1.³⁵ Our study was consistent with these data, revealing that knockdown of HOXA-AS3 notably inhibited G1 arrest in HUVECs through inactivation of CDK2 and Cyclin E1. Frankly speaking, we only focused on the effect of HOXA-AS3 on cell cycle and apoptosis-related proteins so far. Since suppression of Wnt/ β -catenin signaling could inhibit the progression of atherosclerosis,³⁶ we will further investigate the effect of HOXA-AS3 on this signaling pathway.

Taken together, downregulation of HOXA-AS3 significantly suppressed the progression of atherosclerosis via mediation of miR-455-5p/p27 Kip1. Thus, HOXA-AS3

might serve as a potential target for the treatment of atherosclerosis.

Disclosure

The authors declared no competing interests in this research.

References

1. Yue Y, Li Y-Q, Fu S, et al. Osthole inhibits cell proliferation by regulating the TGF- β 1/Smad/p38 signaling pathways in pulmonary arterial smooth muscle cells. *Biomed Pharmacother.* 2020;121:109640. doi:10.1016/j.biopha.2019.109640
2. Miao C, Cao H, Zhang Y, et al. LncRNA DIGIT accelerates tube formation of vascular endothelial cells by sponging miR-134. *Int Heart J.* 2018;59(5):1086–1095. doi:10.1536/ihj.17-290
3. Yan B, Yao J, Liu JY, et al. LncRNA-MIAT regulates microvascular dysfunction by functioning as a competing endogenous RNA. *Circ Res.* 2015;116(7):1143–1156. doi:10.1161/CIRCRESAHA.116.305510
4. Moran M, Cheng X, Ali MS, et al. Transcriptome analysis-identified long noncoding RNA CRNDE in maintaining endothelial cell proliferation, migration, and tube formation. *Sci Rep.* 2019;9(1):19548. doi:10.1038/s41598-019-56030-9

5. Chen L, Yang W, Guo Y, et al. Exosomal lncRNA GAS5 regulates the apoptosis of macrophages and vascular endothelial cells in atherosclerosis. *PLoS One*. 2017;12(9):e0185406. doi:10.1371/journal.pone.0185406
6. Xia WQ, Niu GZ, Yin CG, Lu S, Bu XY. Effects of lncRNA gm4419 on rats with hypertensive cerebral atherosclerosis through NF-kappaB pathway. *Eur Rev Med Pharmacol Sci*. 2019;23(24):10976–10981. doi:10.26355/eurrev_201912_19802
7. Ji Z, Chi J, Sun H, et al. Linc-ROR targets FGF2 to regulate HASMC proliferation and migration via sponging miR-195-5p. *Gene*. 2020;725:144143. doi:10.1016/j.gene.2019.144143
8. Lou X, Ma X, Wang D, et al. Systematic analysis of long non-coding RNA and mRNA expression changes in ApoE-deficient mice during atherosclerosis. *Mol Cell Biochem*. 2019;462(1–2):61–73. doi:10.1007/s11010-019-03610-y
9. Sun G, Li Y, Ji Z. Up-regulation of MIAT aggravates the atherosclerotic damage in atherosclerosis mice through the activation of PI3K/Akt signaling pathway. *Drug Deliv*. 2019;26(1):641–649. doi:10.1080/10717544.2019.1628116
10. Zhu X, Chen D, Liu Y, et al. Long noncoding RNA HOXA-AS3 integrates NF-kappaB signaling to regulate endothelium inflammation. *Mol Cell Biol*. 2019;39(19). doi:10.1128/MCB.00139-19.
11. Wang K, Yang C, Shi J, Gao T. Ox-LDL-induced lncRNA MALAT1 promotes autophagy in human umbilical vein endothelial cells by sponging miR-216a-5p and regulating Beclin-1 expression. *Eur J Pharmacol*. 2019;858:172338. doi:10.1016/j.ejphar.2019.04.019
12. Cui C, Wang X, Shang XM, et al. lncRNA 430945 promotes the proliferation and migration of vascular smooth muscle cells via the ROR2/RhoA signaling pathway in atherosclerosis. *Mol Med Rep*. 2019;19(6):4663–4672. doi:10.3892/mmr.2019.10137
13. Lin S, Zhang R, An X, et al. lncRNA HOXA-AS3 confers cisplatin resistance by interacting with HOXA3 in non-small-cell lung carcinoma cells. *Oncogenesis*. 2019;8(11):60. doi:10.1038/s41389-019-0170-y
14. Okano T, Sato K, Shirai R, et al. Beta-endorphin mediates the development and instability of atherosclerotic plaques. *Int J Endocrinol*. 2020;2020:4139093. doi:10.1155/2020/4139093
15. Zhao H, Liu M, Liu H, Suo R, Lu C. Naringin protects endothelial cells from apoptosis and inflammation by regulating the hippo-YAP pathway. *Biosci Rep*. 2020;40(3). doi:10.1042/BSR20193431
16. Zhu XX, Yan YW, Chen D, et al. Long non-coding RNA HoxA-AS3 interacts with EZH2 to regulate lineage commitment of mesenchymal stem cells. *Oncotarget*. 2016;7(39):63561–63570. doi:10.18632/oncotarget.11538
17. Luo Y, Lu S, Gao Y, et al. Araloside C attenuates atherosclerosis by modulating macrophage polarization via Sirt1-mediated autophagy. *Aging (Albany NY)*. 2020;12(2):1704–1724. doi:10.18632/aging.102708
18. Zhao X, Liu Z, Shen J, et al. microRNA-196a overexpression inhibits apoptosis in hemin-induced K562 cells. *DNA Cell Biol*. 2020;39(2):235–243. doi:10.1089/dna.2019.5061
19. Tong Y, Wang M, Dai Y, et al. lncRNA HOXA-AS3 sponges miR-29c to facilitate cell proliferation, metastasis, and EMT process and activate the MEK/ERK signaling pathway in hepatocellular carcinoma. *Hum Gene Ther Clin Dev*. 2019;30(3):129–141. doi:10.1089/humc.2018.266
20. Helmy HS, Senousy MA, El-Sahar AE, et al. Aberrations of miR-126-3p, miR-181a and Sirtuin1 network mediate Di-(2-ethylhexyl) phthalate-induced testicular damage in rats: the protective role of hesperidin. *Toxicology*. 2020;152406. doi:10.1016/j.tox.2020.152406
21. Lv Y, Duanmu J, Fu X, Li T, Jiang Q. Identifying a new microRNA signature as a prognostic biomarker in colon cancer. *PLoS One*. 2020;15(2):e0228575. doi:10.1371/journal.pone.0228575
22. Xin Y, Wang X, Meng K, et al. Identification of exosomal miR-455-5p and miR-1255a as therapeutic targets for breast cancer. *Biosci Rep*. 2020;40(1). doi:10.1042/BSR20190303.
23. Wang X, Jia Y, Ren J, et al. MicroRNA gga-miR-455-5p suppresses newcastle disease virus replication via targeting cellular suppressors of cytokine signaling 3. *Vet Microbiol*. 2019;239:108460. doi:10.1016/j.vetmic.2019.108460
24. Yang K, Tang XJ, Xu FF, et al. PI3K/mTORC1/2 inhibitor PQR309 inhibits proliferation and induces apoptosis in human glioblastoma cells. *Oncol Rep*. 2020. doi:10.3892/or.2020.7472
25. Jiang T, Chen ZH, Chen Z, Tan D. SULF2 promotes tumorigenesis and inhibits apoptosis of cervical cancer cells through the ERK/AKT signaling pathway. *Braz J Med Biol Res*. 2020;53(2):e8901. doi:10.1590/1414-431x20198901
26. Vaidya K, Jain S, Sahu S, et al. Anticancer agents based on vulnerable components in a signalling pathway. *Mini Rev Med Chem*. 2020. doi:10.2174/1389557520666200212105417
27. Serrya MS, Zaghloul MS. Mycophenolate mofetil attenuates concanavalin A-induced acute liver injury through modulation of TLR4/NF-kappaB and Nrf2/HO-1 pathways. *Pharmacol Rep*. 2020. doi:10.1007/s43440-019-00055-4
28. Choi BK, Fujiwara K, Dayaram T, et al. WIP1 dephosphorylation of p27(Kip1) serine 140 destabilizes p27(Kip1) and reverses anti-proliferative effects of ATM phosphorylation. *Cell Cycle*. 2020;19(4):1–13.
29. Liang Y, Li E, Zhang H, et al. Silencing of lncRNA UCA1 curbs proliferation and accelerates apoptosis by repressing SIRT1 signals by targeting miR-204 in pediatric AML. *J Biochem Mol Toxicol*. 2020;34(3):e22435. doi:10.1002/jbt.22435
30. Zhao J, Xu J, Wang W, et al. Long non-coding RNA LINC-01572:28 inhibits granulosa cell growth via a decrease in p27 (Kip1) degradation in patients with polycystic ovary syndrome. *EBioMedicine*. 2018;36:526–538. doi:10.1016/j.ebiom.2018.09.043
31. Hu Y, Yang Z, Bao D, Ni JS, Lou J. miR-455-5p suppresses hepatocellular carcinoma cell growth and invasion via IGF-1R/AKT/GLUT1 pathway by targeting IGF-1R. *Pathol Res Pract*. 2019;215(12):152674. doi:10.1016/j.prp.2019.152674
32. Hu X, Tan S, Yin H, et al. Selenium-mediated gga-miR-29a-3p regulates LMH cell proliferation, invasion, and migration by targeting COL4A2. *Metallomics*. 2020;12(3):449–459. doi:10.1039/C9MT00266A
33. Liu L, Deng Y, Cai Y, et al. Ablation of Gsa impairs renal tubule proliferation after injury via CDK2/Cyclin E. *Am J Physiol Renal Physiol*. 2020;318(3):F793–F803. doi:10.1152/ajprenal.00367.2019
34. Tian Q, Gu Y, Wang F, et al. Upregulation of miRNA-154-5p prevents the tumorigenesis of osteosarcoma. *Biomed Pharmacother*. 2020;124:109884. doi:10.1016/j.biopha.2020.109884
35. Boratyn E, Nowak I, Karnas E, et al. MCP1 overexpression in human neuroblastoma cell lines causes cell-cycle arrest by G1/S checkpoint block. *J Cell Biochem*. 2020;121(5–6):3406–3425. doi:10.1002/jcb.29614
36. He HQ, Law BYK, Zhang N, et al. Bavachin protects human aortic smooth muscle cells against beta-glycerophosphate-mediated vascular calcification and apoptosis via activation of mTOR-dependent autophagy and suppression of beta-catenin signaling. *Front Pharmacol*. 2019;10:1427. doi:10.3389/fphar.2019.01427

Drug Design, Development and Therapy

Dovepress

Publish your work in this journal

Drug Design, Development and Therapy is an international, peer-reviewed open-access journal that spans the spectrum of drug design and development through to clinical applications. Clinical outcomes, patient safety, and programs for the development and effective, safe, and sustained use of medicines are a feature of the journal, which has also

been accepted for indexing on PubMed Central. The manuscript management system is completely online and includes a very quick and fair peer-review system, which is all easy to use. Visit <http://www.dovepress.com/testimonials.php> to read real quotes from published authors.

Submit your manuscript here: <https://www.dovepress.com/drug-design-development-and-therapy-journal>